Bacteria detect neutrophils via a system that responds to hypochlorous acid and flow

Ilona P. Foik[1,2], Runhang Shu[3], Serena Abbondante[4,5], Summer J. Kasallis[1], Lauren A. Urban[6,7], Andy P. Huang[8], Leora Duong[3], Michaela E. Marshall[4,5], Eric Pearlman[4,5], Timothy L. Downing[6,7,9,*], Albert Siryaporn[1,3,*]

[1]Department of Physics & Astronomy, University of California Irvine, USA.
[2]Institute of Physical Chemistry, Polish Academy of Sciences, Poland.
[3]Department of Molecular Biology & Biochemistry, University of California Irvine, USA.
[4]Department of Ophthalmology, University of California Irvine, USA.
[5]Department of Physiology and Biophysics, University of California Irvine, USA.
[6]Department of Microbiology & Molecular Genetics, University of California Irvine, USA.
[7]Edwards Lifesciences Foundation Cardiovascular Innovation and Research Center, University of California Irvine, USA.
[8]School of Biological Sciences, University of California Irvine, USA
[9]Department of Biomedical Engineering, University of California Irvine, USA.

[*]To which correspondence should be sent:
T. Downing: tim.downing@uci.edu
A. Siryaporn: asiyra@uci.edu

Keywords: neutrophils, shear sensing, hypochlorous acid, *P. aeruginosa*, oxidative stress

ABSTRACT

Neutrophils respond to the presence of bacteria by producing oxidative molecules that are lethal to bacteria, including hypochlorous acid (HOCl). However, the extent to which bacteria detect activated neutrophils or the HOCl that neutrophils produce, has not been understood. Here we report that the opportunistic bacterial pathogen *Pseudomonas aeruginosa* upregulates expression of its *fro* operon in response to stimulated neutrophils. This operon was previously shown to be activated by shear rate of fluid flow in the environment. We show that *fro* is specifically upregulated by HOCl, while other oxidative factors that neutrophils produce including H_2O_2, do not upregulate *fro*. The *fro*-dependent response to HOCl upregulates the expression of multiple methionine sulfoxide reductases, which relieve oxidative stress that would otherwise inhibit growth. Our findings suggest a model in which the detection of shear rate or HOCl activates the *fro* operon, which serves as an early and sensitive host-detection system for *P. aeruginosa* that improves its own survival against neutrophil-mediated host defenses. In support of this model, we found that the *fro* operon is activated in an infection model where flow and neutrophils are present. This response could promote the bacterium's pathogenicity, colonization of tissue, and persistence in infections.

INTRODUCTION

P. aeruginosa is a Gram-negative bacterium that is a major cause of hospital-acquired infections and is a significant antibiotic resistance threat [1]. To survive in a broad range of conditions, this bacterium has evolved signaling pathways that relay information about changes in nutrients, chemical gradients, and mechanical forces such as those generated by fluid flow, and activates responses that promote its survival [2,3]. Understanding how extracellular-sensing pathways detect and respond to host cues is critical for improving treating bacterial infections.

Mammalian host immune systems respond to the presence of bacterial pathogens by recruiting immune cells that migrate rapidly through circulating blood to sites of infection [4]. Neutrophils are the first and most abundant immune cells recruited to inflamed or damaged tissues [5] and are stimulated into an activated state by bacterial components including the membrane constituent lipopolysaccharide. Activated neutrophils produce multiple products that are toxic to bacteria including reactive oxygen species (ROS) and reactive chlorine species (RCS) [6–9]. While the toxic effects of ROS on bacteria are understood, far less is known about how bacteria are affected by RCS [10,11]. Hypochlorous acid (HOCl) is a major neutrophil-produced RCS that is formed through the activity of myeloperoxidase with H_2O_2 and chlorine ions [6,7,12] and is strongly bactericidal [13–15]. *P. aeruginosa* is a potent activator of neutrophil respiratory bursts [16] but whether and how the bacteria detect and respond to these respiratory bursts, is not understood.

P. aeruginosa detects shear rate generated by the flow of fluids via the *fro* operon [3,17], which is upregulated in the bacterium during infection in humans [3,18] (Fig. 1A). In addition, *fro* is necessary for successful colonization of the gastrointestinal tract and lung infections [19,20], although the reasons for its necessity have been unclear. Because flow is ubiquitous in the pulmonary and circulatory systems, in principle the *fro* operon could be upregulated in flow-associated host environments. Given its important role in infection, it is possible that Fro could also respond to other immune-associated cues, such as the presence of neutrophils. The *fro* operon consists of *froABCD* (*PA14_21570*, *PA14_21580, PA14_21590, PA14_21600*), with FroC and FroD predicted to localize to the inner membrane, and FroB predicted to localize in the cytoplasm [21]. Expression of the operon is regulated by the sigma and anti-sigma factors *froR* (*PA14_21550)* and *froI* (*PA14_21560*), respectively [22]. Overexpression of *froR* upregulates *fro,*

whereas overexpression of *froI* downregulates *fro* [3]. Flow activates FroR-dependent transcription of *froABCD* through an unknown mechanism [3].

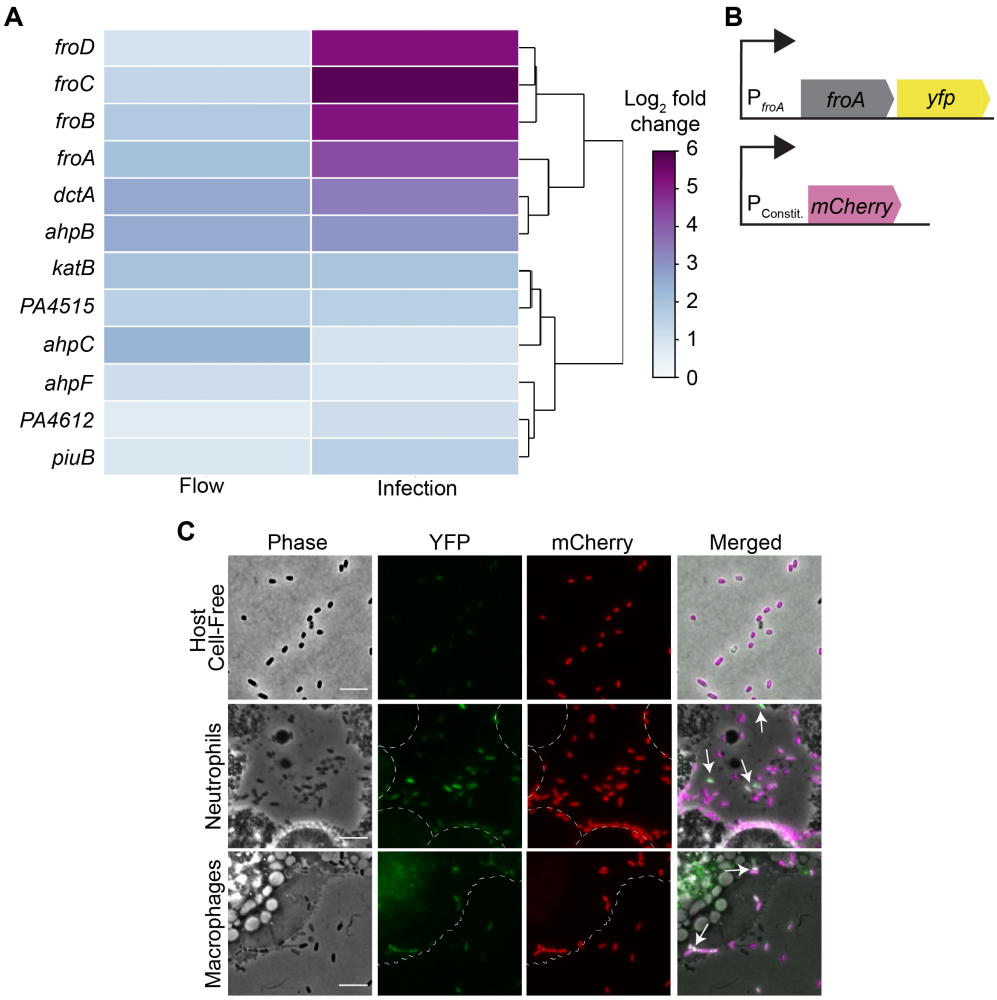

Figure 1. Activation of *fro* promoter transcription by flow and during infection of human tissue. **(A)** RNA-seq heatmap of *P. aeruginosa* genes that are upregulated by at least 3-fold by flow and during infection in human wounds. Datasets are from [3,18]. **(B)** Schematic of a *P. aeruginosa* fluorescent reporter strain that contains a transcriptional fusion of *yfp* to the *fro* promoter and expresses mCherry under a constitutive promoter. **(C)** Representative phase contrast, fluorescence, and merged images of the *P. aeruginosa* reporter strain co-incubated with neutrophils, macrophages, or host cell-free medium. Dashed lines indicate boundaries of the host cells and white arrows indicate *P. aeruginosa* with high YFP/mCherry ratios. Images are representative of three independent experiments. Scale bars represent 5 μm.

We show that the *fro* operon responds directly to HOCl, which is produced by neutrophils during immune response. Using a fluorescent reporter system in live cells and through quantitative measurements of transcription, we show that *fro* expression is upregulated in a mouse model of corneal infection and by activated neutrophils. Through transcriptional profiling, we determine that *fro* upregulation mitigates the toxic effects of HOCl by activating methionine sulfoxide reductases that relieve oxidative

stress in bacteria. These data suggest a novel mechanism by which bacterial defense against host innate immunity is primed by a single system to detect host defense cues through both flow and the presence of the highly potent oxidative factor HOCl.

RESULTS

Host cells stimulate *fro* expression in *P. aeruginosa* under non-flow conditions

We investigated whether the *fro* operon is activated directly by immune cells. To quantify *fro* expression, we used a *P. aeruginosa* strain that co-expresses the yellow fluorescent protein (YFP) under the transcriptional control of the *fro* promoter, and mCherry under the control of a constitutive promoter (Fig. 1B and [3]). While *fro* expression increases under flow (Fig. S1A in the Supplementary Information (SI) and [3]), experiments in this study were performed in the absence of flow in order to deconvolve the effects of flow from potential activation of *fro* by immune cells. Neutrophils and macrophages are among the first immune cells that are recruited to sites of infection. We co-incubated *P. aeruginosa* with neutrophils or macrophages for 30 minutes to determine whether they would elicit a response in the *fro* operon. Relative to *P. aeruginosa* that were incubated in host cell-free media, *P. aeruginosa* in close proximity to human neutrophils or that were engulfed in mouse macrophages appeared to increase *fro* expression (Fig. 1C), suggesting that close proximity to or direct interaction with these host cells stimulate *fro* expression in *P. aeruginosa*.

Activated neutrophils induce *fro* expression

We focused on the potential activation of *fro* expression by neutrophils because *P. aeruginosa* triggers respiratory bursts in neutrophils [16], which generates ROS and RCS. We hypothesized that *fro* activation could be a response to respiratory burst products. *P. aeruginosa* were incubated in conditioned medium in which respiratory bursts were induced in human neutrophils using phorbol myristate acetate (PMA) [23,24] (Fig. 2A). The expression of *fro* was quantified by averaging the ratios of YFP to mCherry fluorescence for at least one hundred individual *P. aeruginosa*. In support of our hypothesis, conditioned medium from PMA-stimulated neutrophils increased expression of *fro* expression by 30-fold compared to conditioned medium from unstimulated neutrophils (Fig. 2B). The increased *fro* expression was not due to

PMA alone, as PMA-treated medium without neutrophils had no effect on *fro* expression (Fig. 2B). Conditioned medium from unstimulated neutrophils had no significant effect on *fro* expression compared to medium alone (Fig. 2B), suggesting that the activation of *fro* is due to the products of respiratory bursts.

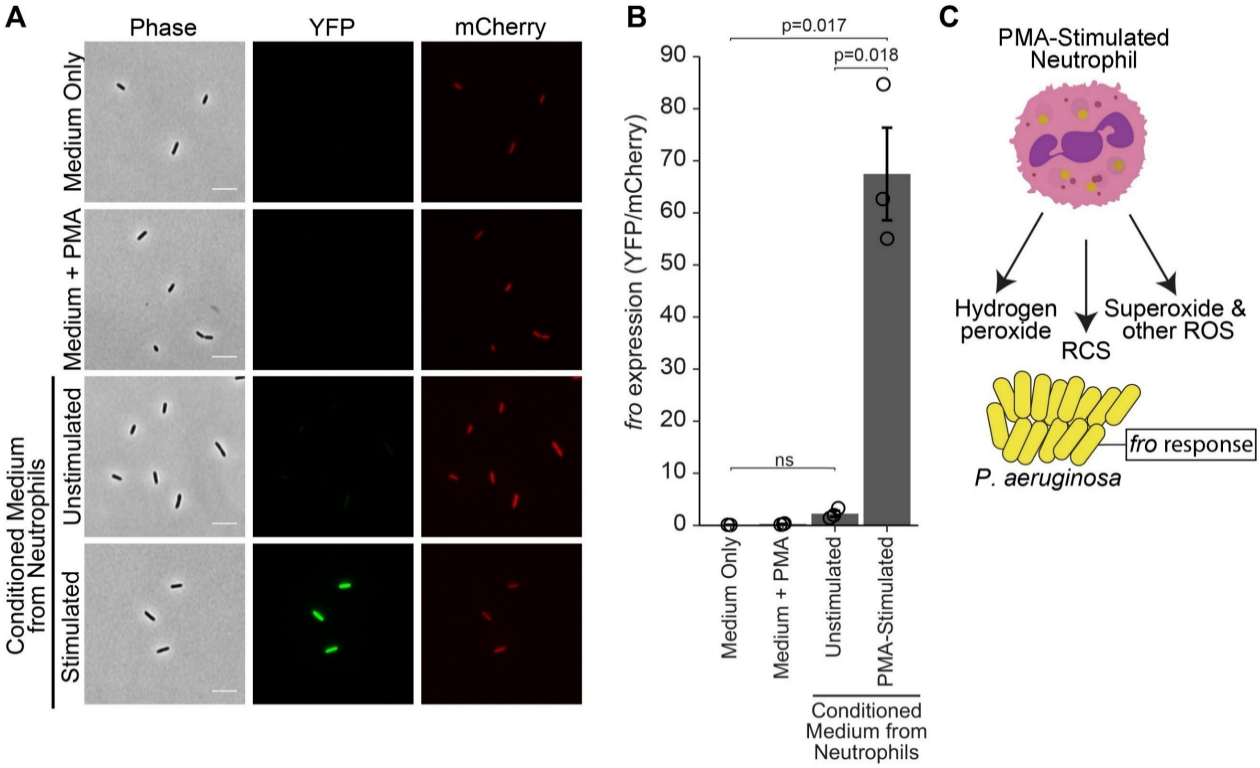

Figure 2. Conditioned medium from stimulated neutrophils induces *fro* expression. **(A)** Representative phase-contrast and fluorescence images and **(B)** *fro* expression as determined by ratios of YFP to mCherry fluorescence, of *P. aeruginosa* that were cultured in medium only, medium with PMA, conditioned medium from PMA-stimulated neutrophils, or conditioned medium from unstimulated neutrophils. Scale bars represent 5 µm. Data points indicate an average from at least one hundred individual *P. aeruginosa*. Gray columns indicate the mean of at least three independent experiments and error bars represent the standard error of the mean (SEM). P-values were obtained using two-tailed t-tests with unequal variances and values of p>0.05 are denoted as ns (nonsignificant). **(C)** Schematic depicting that PMA-stimulated neutrophils produce respiratory burst products that could activate *fro* expression.

HOCl but not H_2O_2 or HNO_3 induces *fro* expression

Activated neutrophils generate ROS and RCS through respiratory bursts (Fig. 2C), which have an inhibitory effect on bacterial growth [6,7,10,13,14]. To explore the hypothesis that these reactive species induce *fro* expression, we measured the effects of NaOCl, H_2O_2, and HNO_3 on *fro* expression at concentrations just below the minimum inhibitory concentrations (MICs) (Fig. 3A-B). NaOCl increased *fro* expression by up 74-fold at 1 µM (Fig. 3B). At 2 µM, NaOCl caused only a 3-fold increase in *fro*

expression but these bacteria were noticeably smaller in size (Fig. S1B in the SI), raising the possibility that the treatment could have interfered with transcription. The activation of *fro* transcription by NaOCl was further assessed using reverse transcription quantitative PCR (RT-qPCR). In support of the *fro-yfp* reporter findings, a 200-fold increase in *fro* transcription was observed using 1 μM NaOCl (Fig. 3C).

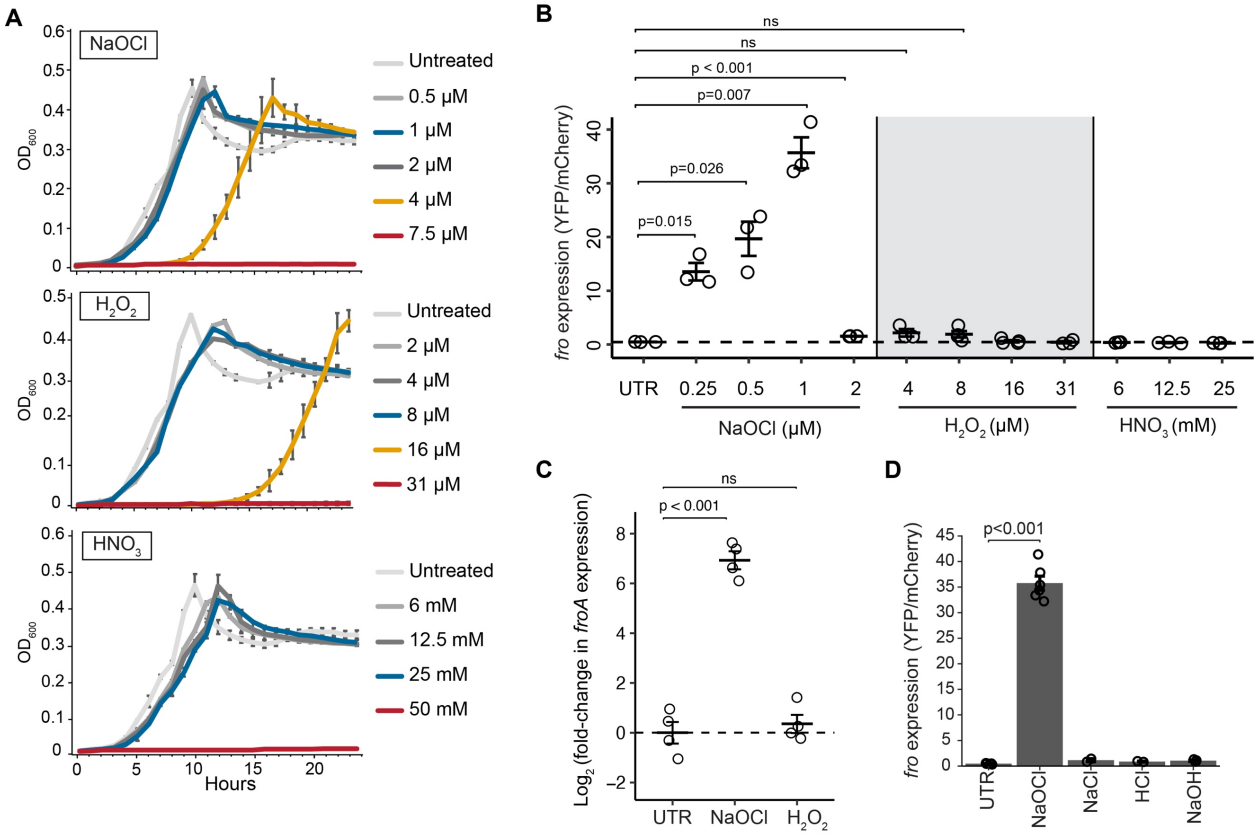

Figure 3. NaOCl but not H_2O_2 or HNO_3 induces *fro* expression.
(A) Growth profiles as measured by optical density (OD_{600}) of *P. aeruginosa* treated with NaOCl, H_2O_2, HNO_3, or no treatment. Data points indicate a mean of at least two independent experiments and error bars indicate SEM. **(B)** *fro* expression as determined by ratios of YFP to mCherry fluorescence in *P. aeruginosa* treated with NaOCl, H_2O_2, or HNO_3, or no treatment (UTR). Horizontal bars indicate the mean of at least three independent experiments and error bars indicate SEM. The dashed line indicates the average YFP/mCherry ratio from the untreated condition. **(C)** Abundance of *fro*A transcripts in *P. aeruginosa* following treatment with 1 μM NaOCl, 4 μM H_2O_2, or no treatment (UTR), as measured by RT-qPCR. Measurements were normalized to 5S ribosomal RNA and the logarithm (base 2) of the fold-change in transcription was computed relative to the untreated condition. Horizontal bars indicate the average of four independent experiments and error bars indicate SEM. **(D)** *fro* expression, measured by YFP to mCherry ratio, in *P. aeruginosa* after treatment with 1 μM NaOCl, 1 μM NaCl, 200 μM HCl, 6 mM NaOH, or no treatment (UTR). Error bars indicate SEM. In panels B and D, data points indicate the average from at least one hundred individual *P. aeruginosa*. P-values were obtained using two-tailed t-tests with unequal variances, with values of p>0.05 denoted as ns.

The increased *fro* expression was not due to sodium or chloride ions alone, as neither NaCl nor HCl affected *fro* expression in the absence of NaOCl (Fig. 3D). The *fro* response to NaOCl was not due to

basic pH, as treatment with up to 6 mM of NaOH had no significant impact on *fro* activation (Fig. 3D). As *fro* activation is not due to sodium or chloride ions, nor changes in pH, we attributed the effects to hypochlorite (OCl^-), which is in equilibrium with the hypochlorous acid species (HOCl) at the pH of 7.1 used in our experiments.

Changes in *fro* expression were assessed using H_2O_2, a strong oxidizer. Small increases in *fro* expression were observed using the subinhibitory concentrations of 4 and 8 μM but these changes were not statistically significant compared to untreated cultures (Fig. 3A-B), and no significant changes in *fro* transcript abundance were observed using qRT-PCR (Fig. 3C). The *fro* response was also assessed using subinhibitory concentrations of HNO_3, for which no change in expression was detected up to near-MIC concentrations (Fig. 3A-B). Together, these results show that Fro expression is activated by HOCl and suggest that HOCl produced by stimulated neutrophils could activate *fro* expression.

Corneal infection activates *fro* expression

P. aeruginosa is a major cause of corneal ulcers and keratitis, which can cause visual impairment and blindness. Neutrophils are recruited within hours to infected corneal epithelia with neutrophil cell density peaking at 18 hours [25]. We tested the hypothesis that *fro* expression is upregulated during infection using a previously-established murine model of corneal infection in which *P. aeruginosa* strain PAO1F is inoculated at the site of a corneal abrasion [26]. Mice corneas were harvested 2 or 20 hours post-infection and *fro* transcripts were quantified using RT-qPCR. Transcription was normalized for number of *P. aeruginosa* using 5S ribosomal RNA. We confirmed that this strain of *P. aeruginosa* upregulates its *fro* transcription in response to NaOCl but not H_2O_2 (Fig. S1B in the SI), consistent with our previous results. In support of the hypothesis, *fro* expression increased significantly by 20 hours post-infection (Fig. 4A). Expression levels showed no significant change within the first two hours following infection, which we attribute to the low level of immune cell recruitment during this period.

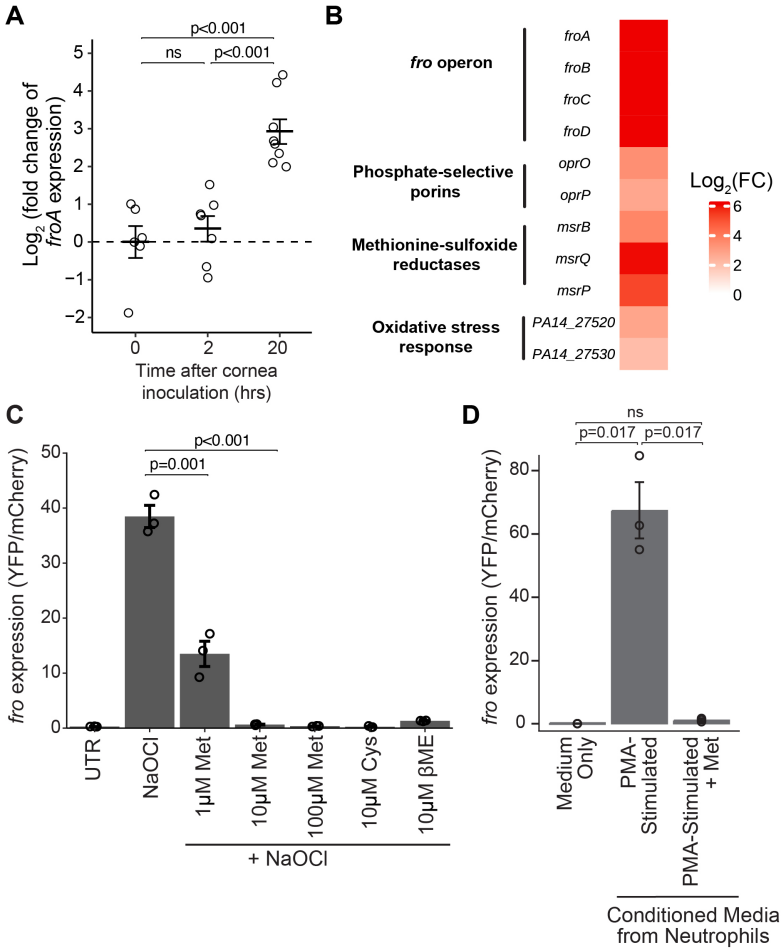

Figure 4. The expression of *fro* is activated during corneal infection and inhibited by methionine and antioxidants.
(A) Abundance of *fro*A transcripts in *P. aeruginosa* 0, 2, or 20 hours after being inoculated on a mouse corneal abrasion, as measured by RT-qPCR. Measurements were normalized to 5S ribosomal RNA and the logarithm (base 2) of the fold-change in transcription was computed relative to the initial inoculum. Data points represent individual experiments. Horizontal bars indicate the average of at least six independent experiments and error bars represent SEM. **(B)** Heatmap showing *P. aeruginosa* gene transcripts that were upregulated by at least 4-fold in wild type compared to the Δ*froR* mutant after treatment with 1 μM NaOCl and that had p-values less than 0.05 (n≥3), sorted by genomic locus. Raw values are in Table S1 in the SI. Log_2(FC) indicates the log_2 of the fold-change. **(C)** *fro* expression, determined by ratios of YFP to mCherry, in *P. aeruginosa* with no treatment (UTR), or treated with 1 μM NaOCl, or 1 μM NaOCl with methionine (Met), cysteine (Cys), or β-mercaptoethanol (βME). **(D)** *fro* expression, determined by ratios of YFP to mCherry, in *P. aeruginosa* after incubation with conditioned medium only (replotted from Fig. 2B), conditioned medium from stimulated neutrophils, or in conditioned medium from stimulated neutrophils with 100 μM methionine. Data points indicate an average from at least one hundred individual *P. aeruginosa*. Gray columns indicate the mean of at least three independent experiments and error bars represent SEM. P-values were obtained using two-tailed t-tests with unequal variances and values of p>0.05 are denoted as ns.

Methionine sulfoxide reductase upregulation requires FroR

To understand how the HOCl response is regulated by *fro*, we performed transcriptional profiling of wild-type (WT) *P. aeruginosa* and a strain containing a deletion of FroR, which is the sigma factor that

is required for *fro* activation [3]. The genes that were most upregulated by NaOCl in WT compared to the Δ*froR* mutant were in the *fro* operon, the phosphate-specific and pyrophosphate-specific outer membrane porin genes *oprO* and *oprP,* and the methionine sulfoxide reductase genes *msrB, msrQ* and *msrP* (Fig. 4B). The methionine sulfoxide reductases (MSRs) have an essential role in bacterial survival and defense against RCS stress. HOCl oxidizes methionine residues 100-fold more rapidly than other cellular components, forming methionine sulfoxide, which impairs protein function [27–31]. MSRs restore proper protein function by reducing methionine sulfoxide back to methionine [11,32]. Our data suggest that *froR* is required for the upregulation of MSRs in response to HOCl stress. It is possible that oxidized methionine increases *fro* expression, which in-turn increases MSR expression.

We reasoned that if oxidized methionine upregulates *fro*, an excess of methionine should inhibit *fro* activation. In support of our interpretation, methionine co-treatment with NaOCl suppressed *fro* expression (Fig. 4C). We hypothesized that if *fro* expression is activated by HOCl oxidation, antioxidants such as cysteine and β-mercaptoethanol (βME) should suppress *fro* activation by functioning as alternative oxidation targets. Indeed, co-treatment of NaOCl with either cysteine or βME significantly suppressed NaOCl-activated *fro* expression (Fig. 4C and Fig. S2 in the SI).

We considered how *fro* could be upregulated by stimulated neutrophils in the context of these findings. RCS produced by neutrophils could oxidize methionine in *P. aeruginosa*, resulting in *fro* upregulation. Under this interpretation, supplying excess methionine should inhibit activation. Indeed, supplementing conditioned media from PMA-stimulated neutrophils with methionine completely suppressed *fro* expression (Fig. 4D). Together, these data suggest a model in which *fro* responds to HOCl-induced oxidation of methionine by upregulating MSRs.

FroR protects *P. aeruginosa* against HOCl

The upregulation of MSRs is expected to improve bacterial growth against HOCl stress. We measured the growth profiles of WT and Δ*froR* strains of *P. aeruginosa*. Treatment with 16 μM NaOCl significantly inhibited the growth of the wild-type strain (Fig. 5A) but resulted in even greater growth inhibition in the Δ*froR* strain. This observation suggests that the *fro* operon improves *P. aeruginosa* tolerance to HOCl stress.

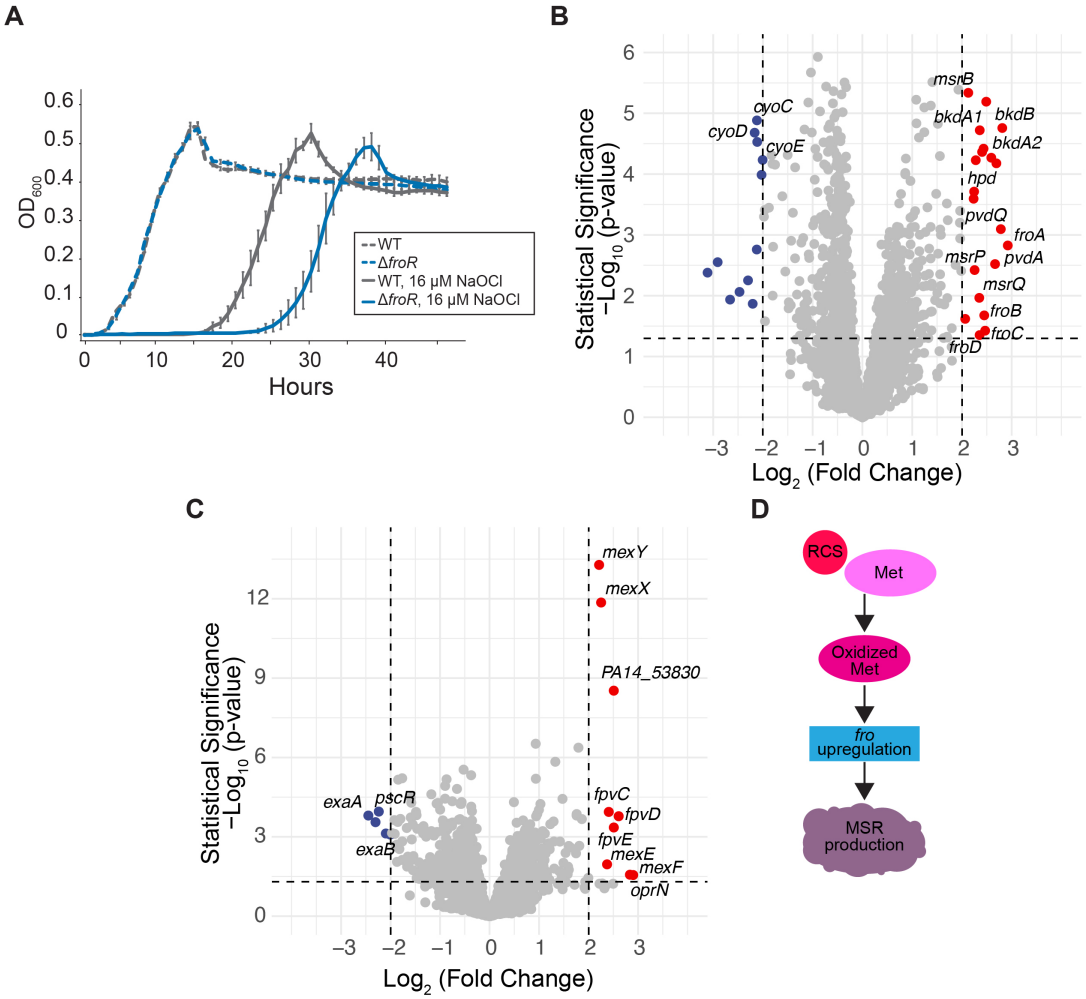

Figure 5. FroR improves *P. aeruginosa* growth against HOCl stress and regulates transcription of genes involved in antioxidant defense.
(A) Growth profiles of wild-type *P. aeruginosa* (WT) and Δ*froR* mutants treated with 16 μM NaOCl or untreated. Data points represent an average of at least three independent experiments and error bars indicate SEM. **(B-C)** Statistical significance as a function of fold-change in transcript abundance in **(B)** WT and **(C)** *ΔfroR P. aeruginosa* after treatment with 1 μM NaOCl (n≥3). Genes in red (upregulated) and blue (downregulated) were altered by at least four-fold (raw values in Table S2-S3 in the SI). The unlabeled genes have not been previously annotated. P-values were determined using the Wald test. Greater values along the vertical axis indicate greater statistical significance and the dashed horizontal line indicates a p-value of 0.05. **(D)** Schematic that depicts a model in which reactive chlorine species (RCS) reacting with methionine (Met) produces oxidized methionine, which upregulates *fro* and in-turn increases the production of methionine sulfoxide reductases.

We considered other genes which may improve WT *P. aeruginosa* tolerance to HOCl. HOCl increased the expression of iron uptake genes (*pvdA* and *pvdQ*) and downregulated the expression of oxidative phosphorylation genes (*cyoCDE*) (Fig. 5B and Table S2 in the SI). These changes suggest that HOCl causes an iron deficiency and decreases oxidative phosphorylation. In order to compensate for decreased oxidative phosphorylation, *P. aeruginosa* may utilize amino acid catabolism as an alternative

energy source, as evidenced by a concomitant upregulation of branched chain amino acid catabolism genes (*hpd, bkdA1, bkdA2,* and *bkdB*) by HOCl (Fig. 5B and Table S2 in the SI).

While the Δ*froR* strain was sensitive to HOCl, the strain was tolerant (Fig. 5A), suggesting that additional mechanisms relieve HOCl stress. In the Δ*froR* mutant, HOCl upregulated genes encoding multidrug efflux pumps (*mexEF-oprN* and *mexXY*) (Fig. 5C and Table S3 in the SI). While these pumps can relieve oxidative stress [33,34], they were not activated in the WT strain. This observation suggests that the response to HOCl may be hierarchical, in which Fro-regulated and Mex pathways could be first-line and second-line responses to HOCl stress, respectively. Supporting this interpretation, it has been reported that treatment of the WT strain using significantly higher (millimolar) HOCl concentrations upregulates *mexEF-oprN* [35] and the *mexXY* regulator *mexT* [36].

DISCUSSION

Neutrophils are activated by the presence of bacteria that infect host tissue. In their activated state, neutrophils generate respiratory bursts that produce an abundance of HOCl. Whether and how bacteria respond to activated neutrophils has not been clear. We have demonstrated that *P. aeruginosa* responds to activated neutrophils by upregulating the transcriptional expression of the *fro* operon, which relieves HOCl stress. Our data suggest that the upregulation of *fro* could function as a bacterial defense mechanism against neutrophil attack, thus improving *P. aeruginosa* survival and colonization of human tissue during infection.

One of the striking features of the *fro* system is that it is finely tuned to activate at sub-lethal concentrations (1-2 μM) of NaOCl. Activated neutrophils produce HOCl concentrations as high as 50 μM [24]. The activation of *fro* at relatively low concentrations suggests that the system functions as an early and sensitive detector of HOCl. In hosts, *fro* may be upregulated in environments where HOCl is present in low concentrations, such as during early stages of neutrophil recruitment in the cornea or when *P. aeruginosa* is spatially distant from activated neutrophils. The early activation of *fro* could benefit *P. aeruginosa* by triggering a protective mechanism before HOCl reaches lethal concentrations. The ability of the Fro system to respond to the presence of fluid flow provides an additional layer of early activation, such as in the case of host circulatory systems. Shear rates that activate *fro* [3] could prime *P. aeruginosa*

defenses against circulating neutrophils. Consistent with this interpretation, shear rate sensitizes Fro to H_2O_2 [17], which is also produced by neutrophils in response to the presence of bacteria [6].

Based on the observations that multi-drug efflux pumps only activate in the absence of FroR and at high HOCl concentrations [35], and that multiple systems repair RCS damage [1–3], the HOCl response is likely to follow a hierarchy of activation. Our data suggest a model in which the *fro* system is the first-line response that suppresses the toxic effects of HOCl towards methionine (Fig. 5D). FroR activates two distinct classes of reductases that repair RCS-oxidized methionine: MsrB reduces methionine sulfoxide with electrons provided by the thioredoxin system [37,38], and MsrPQ uses electrons from the respiratory chain [39]. The activation of both reductase classes enables *P. aeruginosa* to limit RCS stress in both the cytoplasmic and periplasmic spaces by utilizing multiple electron donor sources.

Bacteria that are exposed to low concentrations of HOCl have higher rates of horizontal gene transfer and can acquire antibiotic resistance genes more rapidly [40,41]. The *fro* system could thus facilitate antibiotic resistance through increasing *P. aeruginosa* tolerance to HOCl. Our findings thus suggest that the *fro* pathway could be an important defense mechanism to target in the development of novel antibiotic therapeutics. Inhibition of this pathway could increase *P. aeruginosa* susceptibility to neutrophil-mediated killing while minimizing antibiotic resistance.

MATERIALS AND METHODS

Strains, Growth Conditions, and Reagents

Experiments were performed using the *P. aeruginosa* strain AL143, which is strain PA14 strain that contains the *yfp* gene integrated between *froA* and *froB* and a constitutively-expressed *mCherry* gene [3], Δ*froR* and Δ*froI* mutant strains that were previously constructed [3], and *P. aeruginosa* strain PAO1F[42,43]. Strains were streaked onto LB-Miller (BD Biosciences, Franklin Lakes, NJ) petri dishes containing 2% Bacto agar (BD Biosciences, Franklin Lakes, NJ), incubated overnight at 37 °C, and single colonies were inoculated into 2mL of modified MinA minimal medium (60.3mM K_2HPO_4, 33.0mM KH_2PO4, 7.6mM $(NH_4)_2SO_4$, 1.0mM $MgSO_4$,) [44] containing 0.2% (w/v) sodium citrate as the carbon source. Strains were cultured in MinA minimal medium for 18 hours in a roller drum spinning at 200 rpm

at 37 °C, diluted 1:1000 into fresh MinA minimal medium supplemented with oxidative or antioxidative agents, or were not supplemented and imaged using fluorescence microscopy. *P. aeruginosa* cultures were incubated with NaOCl, H_2O_2, HNO_3 for 3 hours unless otherwise stated at 37 °C before imaging.

Neutrophils were isolated from blood samples from healthy donors between 18 to 65 years old that were collected at the Institute for Clinical and Translational Science at the University of California, Irvine, through approved protocols with the UCI Institutional Review Board HS#2001-2058, and informed consent was obtained from all donors. Neutrophils were prepared as described in [45]. Briefly, 3% dextran (from Leuconostoc spp, M_r 450,000-650,000, Sigma-Aldrich, St. Louis, MO) in PBS (Gibco, ThermoFisher, Waltham, MA) was used to separate red blood cells (RBCs) from whole blood. Neutrophils were purified from the remaining cells by overlaying on a Ficoll density gradient (GE Healthcare, Chicago, IL) following centrifugation in Ficoll-Paque Centrifugation Media (GE Healthcare, Chicago, IL) for 25 minutes at 500 × g. The remaining RBCs were lysed using RBC Lysis Buffer (Fisher Scientific, Hampton, NH), and neutrophils were resuspended in RPMI 1640 medium (ATCC, Manassas, VA) and purity was assessed by flow cytometry using the ACEA NovoCyte Flow Cytometer and fluorescent antibodies APC-CD11b, FITC-CD16 and PE-CD66b (eBioscience, San Diego, CA). Neutrophils were immediately used for neutrophil stimulation or co-incubation experiments with *P. aeruginosa*. This procedure routinely yielded greater than 95% CD11B-positive neutrophil populations.

J774.1 mouse macrophages (ATCC) were cultured in 10 mL DMEM (Gibco, ThermoFisher) in T75 flasks (VWR, Radnor, PA) at 37 °C with 5% CO_2. Macrophages were passaged every three days through scraping and were passaged every 5 days through trypsinization.

For *P. aeruginosa* size analysis experiments, cultures were incubated at 37 °C in 250 mL flasks for 3 hours with shaking at 225 rpm following the 1:1000 dilution. For methionine and antioxidant treatments, following the 1:1000 dilution, cultures were supplemented with NaOCl and the addition of methionine, β-mercaptoethanol (βME) or cysteine. 50 mL of each bacterial culture was incubated at 37 °C in 250 mL flasks for 3 hours with shaking at 225 rpm, imaged, and analyzed as described in the fluorescence microscopy section.

Fluorescence and Phase Contrast Microscopy

Bacteria were immobilized on 1% agarose pads containing minimal medium and imaged immediately. Cultures containing densities below 10 *P. aeruginosa* per frame were concentrated using a syringe filter with 0.2 or 0.8 μm pore sizes (Millipore, Burlington, MA). Images were acquired using a Nikon Eclipse Ti-E microscope (Nikon, Melville, NY) containing a Nikon 100X Plan Apo (1.45 N.A.) objective, a Nikon Ph3 phase contrast condenser annulus, a Sola light engine (Lumencor, Beaverton, OR), an LED-DA/FI/TX filter set (Semrock, Rochester, NY) for visualizing the mCherry fluorescence spectrum containing a 409/493/596 dichroic and 575/25 nm filters for excitation and 641/75 nm filters for emission, an LED-CFP/YFP/MCHERRY filter set (Semrock) for visualizing YFP fluorescence containing a 459/526/596 dichroic and 509/22 nm filters for excitation and 544/24 nm filters for emission, and a Hamamatsu Orca Flash 4.0 V2 camera (Hamamatsu, Bridgewater, NJ).

Images were acquired using Nikon NIS-Elements and analyzed using custom built software written previously [46] in Matlab (Mathworks, Natick, MA). See the "Data, code, and materials availability" section below to download code. Briefly, *P. aeruginosa* masks were determined from phase contrast images using an edge-detection algorithm. For size analysis, the total pixel area of each individual *P. aeruginosa* was determined by computing the mask area and converting from pixels to μm^2 by multiplying the mask area by a factor of 0.004225 μm^2/pixel to account for the microscope camera pixel size and objective magnification. *Fro* expression was quantified by averaging computed ratios of YFP to mCherry fluorescence for at least one hundred individual *P. aeruginosa*. In each experiment, a minimum of 100 *P. aeruginosa* were imaged and used for analysis in which ratios were computed from the masked areas. To image *P. aeruginosa* under flow, microfluidic devices were fabricated using standard soft lithography techniques as established previously [47] with channel dimensions of 100 μm x 50 μm (width x height) and a flow rate of approximately 5 μL/min.

Co-incubation of Mammalian Cells with *P. aeruginosa*

P. aeruginosa were cultured for 18 hours in minimal medium, centrifuged at 4600 x g for 2 minutes and resuspended in DPBS (Gibco, ThermoFisher) three times, and diluted to a final OD_{600} of 0.2. Macrophages that were harvested from growth flasks or freshly prepared neutrophils were washed three times by centrifuging at 300 x g for 5 minutes and resuspending in DPBS, and 1 mL aliquots containing $4x10^5$ cells/mL were transferred into flat-bottom dishes. *P. aeruginosa* culture was added to the cells at a

multiplicity of infection of 10 and incubated at 37 °C with CO_2 for 30 minutes. Dishes were aspirated until approximately 20 µL of medium remained and pads consisting of 1% agarose containing DPBS were placed on top of the samples in the dishes to immobilize bacteria and cells. Samples were imaged immediately using microscopy.

Conditioned Medium from Neutrophils

Approximately $2x10^6$/mL of freshly harvested neutrophils were incubated at 37 °C in a roller drum spinning at a speed of 4 rotations per minute in PBGT medium (10 mM phosphate buffer pH 7.4 (2.46 mM monobasic with 7.54 mM dibasic sodium phosphate) containing 140 mM sodium chloride, 10 mM potassium chloride, 0.5 mM magnesium chloride, 1 mM calcium chloride, 1 mg/mL glucose, and 5 mM taurine [24]). To activate neutrophils, cultures were supplemented with 100 ng/mL of PMA for 1 hour and were separated from the supernatant by centrifugation for 5 minutes at 4,600 x g and 25 °C. The supernatant was isolated and used as conditioned medium. *P. aeruginosa* cultures were incubated for 3 hours in conditioned medium at 37 °C before imaging.

Growth Curves

Growth curve experiments were performed using a Synergy HTX multi-mode plate reader and sterile, tissue-culture treated, clear bottom, black polystyrene 96-well microplates (Corning, Corning, NY) containing 200 µL of culture in each well. The temperature set point was 37 °C and preheated before beginning measurements. For experiments performed with stationary phase bacteria, overnight cultures of bacteria were grown for 18 hours at 37 °C in the roller drum at 200 rpm to saturation, diluted into minimal medium to an optical density at 600 nm (OD_{600}) of 0.01 containing NaOCl, H_2O_2, HNO_3 or no supplement. Plates were incubated at 37 °C with continuous orbital shaking with an amplitude of 3 mm at the frequency of 180 cycles per minute and measured for OD_{600} every 20 minutes.

Reverse Transcription Quantitative PCR (RT-qPCR)

Strains were cultured overnight, diluted 1:1000 into MinA medium, incubated in a shaker at 225 rpm at 37°C for 2.5 hours, treated with 1 µM NaOCl, 4 µM H_2O_2, or untreated for 30 minutes, concentrated using syringe filters, and centrifuged at 13,000 × g for 4 minutes to pellet *P. aeruginosa*. Pellets were either snap-frozen in liquid nitrogen or processed immediately for RNA extraction using the

NucleoSpin RNA kit (Macherey-Nagel, Allentown, PA). cDNA was prepared using the High-Capacity cDNA Reverse Transcriptase Kit (ThermoFisher). Quantitative PCR was performed using the SsoAdvanced Universal SYBR Green Supermix (BioRad, Hercules, CA) using the C1000 Thermal Cycler with a CFX96 real-time detection system (Bio-Rad). *froA* transcripts were quantified using the primers 5'-TTTCCCTCGCTTCCTCCGTC-3' and 5'-ACCTTCCTTGGCCTTCTCGG-3', which target PA14_21570 or PA3284 in PA14 or PAO1, respectively. The transcript abundance for each sample was normalized by 5S rRNA abundance, which was determined using the primers 5'-TAGAGCGTTGGAACCACCTG-3' and 5'-GAGACCCCACACTACCATCG-3' [48], yielding normalized count thresholds (Cts). The average fold change in transcript abundance was determined by computing the ratio of the averaged normalized Cts and raising by the power of 2, as performed previously [49].

Murine Model of Corneal Infection

The expression of *froA* was assessed in a murine model of corneal infection as described previously[50,51]. Briefly, *P. aeruginosa* strain PAO1F was cultured to mid-exponential phase in modified MinA minimal medium containing 0.05% citrate, 0.1% casamino acids (Gibco) and 0.2% glucose as the carbon sources and resuspended in PBS (Gibco). Corneal epithelia of C57BL/6J mice aged 6-8 weeks (Jackson Laboratory, Bar Harbor, ME) were abraded with 3x5 mm scratches using a 25 g needle, and 2 µL of PBS containing $5x10^4$ of *P. aeruginosa* strain PAO1F was applied topically. Comparable numbers of male and female mice were used in each experimental group. Mouse eyeballs were collected and homogenized in 1 mL PBS at 2 hours post infection or 20 hours post infection. The homogenate was centrifuged for 5 minutes at 150 x g to remove corneal materials. Supernatant was centrifuged for 4 minutes at 13,000 x g. Pellets were suspended in lysis solution (10 mM Tris-HCl, 1 mM EDTA pH 8.0, 0.5 mg/mL lysozyme, 1% SDS) [49]. RNA was prepared using the NucleoSpin RNA kit (Macherey-Nagel) and assessed for mRNA expression using RT-qPCR.

RNA-seq Library Preparation and Data Analysis

P. aeruginosa was cultured and RNA was prepared as described in the RT-qPCR section. RNA yield was measured using a Nanodrop 2000 (Thermo Fisher, Waltham, MA). Samples were depleted of ribosomal RNA using the NEBNext rRNA Depletion kit (New Enland Biolabs, Ipswich, MA), from which cDNA libraries were constructed using the NEBNext Ultra II Directional Library kit (NEB), which were

sequenced by the UC Irvine Genomics Research & Technology Hub (Irvine, CA) using an Illumina NovaSeq X Plus (Illumina, San Diego, CA) using paired-end 150 bp reads at a depth of approximately 10 M read per sample. Raw reads were checked with fastQC [52] (version 0.21.1), and trimmed and filtered into paired and unpaired reads using Trimmomatic [53] (version 0.39) in Java (1.8.0) using the 'PE' setting. Paired and unpaired reads were aligned to the PA14 genome (NCBI accession NC_008463.1) using Bowtie2 [54] (version 2.5.4) using the default 'sensitive' mode, were counted using the featureCounts program in Subread [55] (version 2.0.8) with the 'countReadPairs' option enabled for paired-end reads, and were fit into a negative binomial model to compute fold-change in gene expression using DeSeq2 [56] (version 1.40.2). The statistical significance of the changes were computed using the Wald test in DeSeq2. Gene Ontology enrichment analysis for Fig. 1A was performed using GOEnrichment [57] (version 2.0.1). The *msrQ* (PA14_62100), *msrP* (PA14_62110) genes were annotated at Pseudomonas.com [21] as *yedZ* and *yedY*, respectively, but are referred to here with their updated names [58].

Statistical Analysis

Statistical analysis and figures were generated in R (The R Foundation, Vienna, Austria) (version 4) and RStudio (Posit Software, Boston, MA).

Data, Code and Materials Availability

Raw data for all figures that contain statistical analyses are available in the Supplementary Information Source Data file. RNA-seq data is available at the National Center for Biotechnology Information Gene Expression Omnibus (GEO) (accession number GSE290217, *accessible during review period using the token: whcbicwsvnmjdqj*). The custom Matlab scripts used to process and analyze fluorescence microscopy data are freely available at https://github.com/asirya/AVIassembleGUI.

ACKNOWLEDGEMENTS

The authors thank Michael Z. Zulu and Stephanie Matsuno for their feedback on prior drafts of this article, Hew Yeng Lai for imaging of bacteria in microfluidic devices, and Hanjuan Shao for assistance with RNA preparation.

Author Contributions: I.P.F., R.S. and A.S. conceived and designed the experiments. L.A.U. prepared neutrophils from human samples. S.A. and M.E.M. performed mouse corneal infection experiments and L.D. homogenized tissue. A.H. performed growth curves. S.J.K. prepared cDNA libraries from RNA samples for RNA-seq. R.S. performed RT-qPCR experiments and analyzed RNA-seq data. I.P.F. performed all other experiments and analyzed data. I.P.F. and L.A.U. wrote the initial draft of the manuscript. S.J.K., R.S. and A.S. revised it. All authors edited the paper.

Funding: This work was supported by the Stanley Behrens Fellows in Medicine Award to L.U., and grants from the National Institutes of Health (NIH) National Institute of Biomedical Imaging and Bioengineering (NIBIB) (R21EB027840-01), the National Cancer Institute (NCI) (DP2CA250382-01), the National Science Foundation (NSF) (DMS1763272), and the Simons Foundation (594598QN) to T.L.D. I.P.F received funding from the Horizon Europe Research and Innovation Program through the Marie Skłodowska-Curie grant #847413 and from the Program of the Ministry of Science and Higher Education #5005/H2020-MSCA-COFUND/2019/2.

Competing Interest Statement: Authors declare that they have no competing interests.

REFERENCES

[1] Centers for Disease Control and Prevention (U.S.), Antibiotic resistance threats in the United States, 2019, Centers for Disease Control and Prevention (U.S.), 2019. https://doi.org/10.15620/cdc:82532.

[2] F.C. Fang, E.R. Frawley, T. Tapscott, A. Vázquez-Torres, Bacterial Stress Responses during Host Infection, Cell Host Microbe 20 (2016) 133–143. https://doi.org/10.1016/j.chom.2016.07.009.

[3] J.E. Sanfilippo, A. Lorestani, M.D. Koch, B.P. Bratton, A. Siryaporn, H.A. Stone, Z. Gitai, Microfluidic-based transcriptomics reveal force-independent bacterial rheosensing, Nat Microbiol 4 (2019) 1274–1281. https://doi.org/10.1038/s41564-019-0455-0.

[4] K. Aymonnier, J. Amsler, P. Lamprecht, A. Salama, V. Witko-Sarsat, The neutrophil: A key resourceful agent in immune-mediated vasculitis, Immunol Rev 314 (2023) 326–356. https://doi.org/10.1111/imr.13170.

[5] E.G. Lavoie, T. Wangdi, B.I. Kazmierczak, Innate immune responses to Pseudomonas aeruginosa infection, Microbes Infect 13 (2011) 1133–1145. https://doi.org/10.1016/j.micinf.2011.07.011.

[6] A.W. Segal, How neutrophils kill microbes, Annu Rev Immunol 23 (2005) 197–223. https://doi.org/10.1146/annurev.immunol.23.021704.115653.

[7] M.B. Hampton, A.J. Kettle, C.C. Winterbourn, Inside the neutrophil phagosome: oxidants, myeloperoxidase, and bacterial killing, Blood 92 (1998) 3007–3017.

[8] A. Ulfig, L.I. Leichert, The effects of neutrophil-generated hypochlorous acid and other hypohalous acids on host and pathogens, Cell Mol Life Sci (2020). https://doi.org/10.1007/s00018-020-03591-y.

[9] S. Sultana, A. Foti, J.-U. Dahl, Bacterial Defense Systems against the Neutrophilic Oxidant Hypochlorous Acid, Infect Immun 88 (2020) e00964-19. https://doi.org/10.1128/IAI.00964-19.

[10] F.C. Fang, Antimicrobial actions of reactive oxygen species, mBio 2 (2011). https://doi.org/10.1128/mBio.00141-11.

[11] M.J. Gray, W.-Y. Wholey, U. Jakob, Bacterial responses to reactive chlorine species, Annu Rev Microbiol 67 (2013) 141–160. https://doi.org/10.1146/annurev-micro-102912-142520.

[12] J.E. Harrison, J. Schultz, Studies on the chlorinating activity of myeloperoxidase, J Biol Chem 251 (1976) 1371–1374.

[13] C. Estrela, R.G. Ribeiro, C.R.A. Estrela, J.D. Pécora, M.D. Sousa-Neto, Antimicrobial effect of 2% sodium hypochlorite and 2% chlorhexidine tested by different methods, Braz Dent J 14 (2003) 58–62. https://doi.org/10.1590/s0103-64402003000100011.

[14] J.M. Albrich, J.K. Hurst, Oxidative inactivation of Escherichia coli by hypochlorous acid. Rates and differentiation of respiratory from other reaction sites, FEBS Lett 144 (1982) 157–161. https://doi.org/10.1016/0014-5793(82)80591-7.

[15] C.C. Winterbourn, A.J. Kettle, M.B. Hampton, Reactive Oxygen Species and Neutrophil Function, Annu Rev Biochem 85 (2016) 765–792. https://doi.org/10.1146/annurev-biochem-060815-014442.

[16] E.T. Jensen, A. Kharazmi, K. Lam, J.W. Costerton, N. Høiby, Human polymorphonuclear leukocyte response to Pseudomonas aeruginosa grown in biofilms, Infect Immun 58 (1990) 2383–2385. https://doi.org/10.1128/iai.58.7.2383-2385.1990.

[17] G.C. Padron, A.M. Shuppara, A. Sharma, M.D. Koch, J.-J.S. Palalay, J.N. Radin, T.E. Kehl-Fie, J.A. Imlay, J.E. Sanfilippo, Shear rate sensitizes bacterial pathogens to H2O2 stress, Proc Natl Acad Sci U S A 120 (2023) e2216774120. https://doi.org/10.1073/pnas.2216774120.

[18] D.M. Cornforth, J.L. Dees, C.B. Ibberson, H.K. Huse, I.H. Mathiesen, K. Kirketerp-Møller, R.D. Wolcott, K.P. Rumbaugh, T. Bjarnsholt, M. Whiteley, Pseudomonas aeruginosa transcriptome during human infection, Proc Natl Acad Sci U S A 115 (2018) E5125–E5134. https://doi.org/10.1073/pnas.1717525115.

[19] E. Potvin, D.E. Lehoux, I. Kukavica-Ibrulj, K.L. Richard, F. Sanschagrin, G.W. Lau, R.C. Levesque, In vivo functional genomics of Pseudomonas aeruginosa for high-throughput screening of new virulence factors and antibacterial targets, Environ Microbiol 5 (2003) 1294–1308. https://doi.org/10.1046/j.1462-2920.2003.00542.x.

[20] D. Skurnik, D. Roux, H. Aschard, V. Cattoir, D. Yoder-Himes, S. Lory, G.B. Pier, A comprehensive analysis of in vitro and in vivo genetic fitness of Pseudomonas aeruginosa using high-throughput sequencing of transposon libraries, PLoS Pathog 9 (2013) e1003582. https://doi.org/10.1371/journal.ppat.1003582.

[21] G.L. Winsor, E.J. Griffiths, R. Lo, B.K. Dhillon, J.A. Shay, F.S.L. Brinkman, Enhanced annotations and features for comparing thousands of Pseudomonas genomes in the Pseudomonas genome database, Nucleic Acids Res 44 (2016) D646-653. https://doi.org/10.1093/nar/gkv1227.

[22] A.L. Boechat, G.H. Kaihami, M.J. Politi, F. Lépine, R.L. Baldini, A novel role for an ECF sigma factor in fatty acid biosynthesis and membrane fluidity in Pseudomonas aeruginosa, PLoS One 8 (2013) e84775. https://doi.org/10.1371/journal.pone.0084775.

[23] A. Karlsson, J.B. Nixon, L.C. McPhail, Phorbol myristate acetate induces neutrophil NADPH-oxidase activity by two separate signal transduction pathways: dependent or independent of phosphatidylinositol 3-kinase, J Leukoc Biol 67 (2000) 396–404. https://doi.org/10.1002/jlb.67.3.396.

[24] J.M. Dypbukt, C. Bishop, W.M. Brooks, B. Thong, H. Eriksson, A.J. Kettle, A sensitive and selective assay for chloramine production by myeloperoxidase, Free Radic Biol Med 39 (2005) 1468–1477. https://doi.org/10.1016/j.freeradbiomed.2005.07.008.

[25] Z. Li, A.R. Burns, C.W. Smith, Two waves of neutrophil emigration in response to corneal epithelial abrasion: distinct adhesion molecule requirements, Invest Ophthalmol Vis Sci 47 (2006) 1947–1955. https://doi.org/10.1167/iovs.05-1193.

[26] M.S. Minns, K. Liboro, T.S. Lima, S. Abbondante, B.A. Miller, M.E. Marshall, J. Tran Chau, A. Roistacher, A. Rietsch, G.R. Dubyak, E. Pearlman, NLRP3 selectively drives IL-1β secretion by Pseudomonas aeruginosa infected neutrophils and regulates corneal disease severity, Nat Commun 14 (2023) 5832. https://doi.org/10.1038/s41467-023-41391-7.

[27] C.C. Winterbourn, Comparative reactivities of various biological compounds with myeloperoxidase-hydrogen peroxide-chloride, and similarity of the oxidant to hypochlorite, Biochim Biophys Acta 840 (1985) 204–210. https://doi.org/10.1016/0304-4165(85)90120-5.

[28] C.L. Hawkins, D.I. Pattison, M.J. Davies, Hypochlorite-induced oxidation of amino acids, peptides and proteins, Amino Acids 25 (2003) 259–274. https://doi.org/10.1007/s00726-003-0016-x.

[29] D.I. Pattison, M.J. Davies, Reactions of myeloperoxidase-derived oxidants with biological substrates: gaining chemical insight into human inflammatory diseases, Curr Med Chem 13 (2006) 3271–3290. https://doi.org/10.2174/092986706778773095.

[30] G. Atmaca, Antioxidant effects of sulfur-containing amino acids, Yonsei Med J 45 (2004) 776–788. https://doi.org/10.3349/ymj.2004.45.5.776.

[31] P. Bin, R. Huang, X. Zhou, Oxidation Resistance of the Sulfur Amino Acids: Methionine and Cysteine, Biomed Res Int 2017 (2017) 9584932. https://doi.org/10.1155/2017/9584932.

[32] H.B. Chandra, A. Shome, R. Sahoo, S. Apoorva, S.K. Bhure, M. Mahawar, Periplasmic methionine sulfoxide reductase (MsrP)-a secondary factor in stress survival and virulence of Salmonella Typhimurium, FEMS Microbiol Lett 370 (2023) fnad063. https://doi.org/10.1093/femsle/fnad063.

[33] S. Fraud, K. Poole, Oxidative stress induction of the MexXY multidrug efflux genes and promotion of aminoglycoside resistance development in Pseudomonas aeruginosa, Antimicrob Agents Chemother 55 (2011) 1068–1074. https://doi.org/10.1128/AAC.01495-10.

[34] E. Fargier, M. Mac Aogáin, M.J. Mooij, D.F. Woods, J.P. Morrissey, A.D.W. Dobson, C. Adams, F. O'Gara, MexT functions as a redox-responsive regulator modulating disulfide stress resistance in Pseudomonas aeruginosa, J Bacteriol 194 (2012) 3502–3511. https://doi.org/10.1128/JB.06632-11.

[35] K.V. Farrant, L. Spiga, J.C. Davies, H.D. Williams, Response of Pseudomonas aeruginosa to the Innate Immune System-Derived Oxidants Hypochlorous Acid and Hypothiocyanous Acid, J Bacteriol 203 (2020) e00300-20. https://doi.org/10.1128/JB.00300-20.

[36] B. Groitl, J.-U. Dahl, J.W. Schroeder, U. Jakob, Pseudomonas aeruginosa defense systems against microbicidal oxidants, Mol Microbiol 106 (2017) 335–350. https://doi.org/10.1111/mmi.13768.

[37] B. Ezraty, L. Aussel, F. Barras, Methionine sulfoxide reductases in prokaryotes, Biochim Biophys Acta 1703 (2005) 221–229. https://doi.org/10.1016/j.bbapap.2004.08.017.

[38] S. Lourenço Dos Santos, I. Petropoulos, B. Friguet, The Oxidized Protein Repair Enzymes Methionine Sulfoxide Reductases and Their Roles in Protecting against Oxidative Stress, in Ageing and in Regulating Protein Function, Antioxidants (Basel) 7 (2018) 191. https://doi.org/10.3390/antiox7120191.

[39] A. Gennaris, B. Ezraty, C. Henry, R. Agrebi, A. Vergnes, E. Oheix, J. Bos, P. Leverrier, L. Espinosa, J. Szewczyk, D. Vertommen, O. Iranzo, J.-F. Collet, F. Barras, Repairing oxidized proteins in the bacterial envelope using respiratory chain electrons, Nature 528 (2015) 409–412. https://doi.org/10.1038/nature15764.

[40] A.-M. Hou, D. Yang, J. Miao, D.-Y. Shi, J. Yin, Z.-W. Yang, Z.-Q. Shen, H.-R. Wang, Z.-G. Qiu, W.-L. Liu, J.-W. Li, M. Jin, Chlorine injury enhances antibiotic resistance in Pseudomonas aeruginosa through over expression of drug efflux pumps, Water Res 156 (2019) 366–371. https://doi.org/10.1016/j.watres.2019.03.035.

[41] M. Jin, L. Liu, D. Wang, D. Yang, W. Liu, J. Yin, Z. Yang, H. Wang, Z. Qiu, Z. Shen, D. Shi, H. Li, J. Guo, J. Li, Chlorine disinfection promotes the exchange of antibiotic resistance genes across bacterial genera by natural transformation, ISME J 14 (2020) 1847–1856. https://doi.org/10.1038/s41396-020-0656-9.

[42] C. Vareechon, S.E. Zmina, M. Karmakar, E. Pearlman, A. Rietsch, Pseudomonas aeruginosa Effector ExoS Inhibits ROS Production in Human Neutrophils, Cell Host Microbe 21 (2017) 611-618.e5. https://doi.org/10.1016/j.chom.2017.04.001.

[43] R.E. Vance, A. Rietsch, J.J. Mekalanos, Role of the type III secreted exoenzymes S, T, and Y in systemic spread of Pseudomonas aeruginosa PAO1 in vivo, Infect Immun 73 (2005) 1706–1713. https://doi.org/10.1128/IAI.73.3.1706-1713.2005.

[44] H. Malke, Jeffrey H. Miller, A Short Course in Bacterial Genetics – A Laboratory Manual and Handbook forEscherichia coli and Related Bacteria. Cold Spring Harbor 1992. Cold Spring Harbor Laboratory Press. ISBN: 0–87969-349–5, J Basic Microbiol 33 (1993) 278–278. https://doi.org/10.1002/jobm.3620330412.

[45] H.L. Clark, S. Abbondante, M.S. Minns, E.N. Greenberg, Y. Sun, E. Pearlman, Protein Deiminase 4 and CR3 Regulate Aspergillus fumigatus and β-Glucan-Induced Neutrophil Extracellular Trap Formation, but Hyphal Killing Is Dependent Only on CR3, Front Immunol 9 (2018) 1182. https://doi.org/10.3389/fimmu.2018.01182.

[46] T. Doolin, H.M. Amir, L. Duong, R. Rosenzweig, L.A. Urban, M. Bosch, A. Pol, S.P. Gross, A. Siryaporn, Mammalian histones facilitate antimicrobial synergy by disrupting the bacterial proton gradient and chromosome organization, Nat Commun 11 (2020) 3888. https://doi.org/10.1038/s41467-020-17699-z.

[47] A. Siryaporn, M.K. Kim, Y. Shen, H.A. Stone, Z. Gitai, Colonization, competition, and dispersal of pathogens in fluid flow networks, Curr Biol 25 (2015) 1201–1207. https://doi.org/10.1016/j.cub.2015.02.074.

[48] S.K. Chuang, G.D. Vrla, K.S. Fröhlich, Z. Gitai, Surface association sensitizes Pseudomonas aeruginosa to quorum sensing, Nat Commun 10 (2019) 4118. https://doi.org/10.1038/s41467-019-12153-1.

[49] J.-L. Bru, B. Rawson, C. Trinh, K. Whiteson, N.M. Høyland-Kroghsbo, A. Siryaporn, PQS Produced by the Pseudomonas aeruginosa Stress Response Repels Swarms Away from Bacteriophage and Antibiotics, J Bacteriol 201 (2019) e00383-19. https://doi.org/10.1128/JB.00383-19.

[50] Y. Sun, M. Karmakar, P.R. Taylor, A. Rietsch, E. Pearlman, ExoS and ExoT ADP Ribosyltransferase Activities Mediate *Pseudomonas aeruginosa* Keratitis by Promoting Neutrophil Apoptosis and Bacterial Survival, The Journal of Immunology 188 (2012) 1884–1895. https://doi.org/10.4049/jimmunol.1102148.

[51] M.S. Minns, K. Liboro, T.S. Lima, S. Abbondante, B.A. Miller, M.E. Marshall, J. Tran Chau, A. Roistacher, A. Rietsch, G.R. Dubyak, E. Pearlman, NLRP3 selectively drives IL-1β secretion by Pseudomonas aeruginosa infected neutrophils and regulates corneal disease severity, Nat Commun 14 (2023) 5832. https://doi.org/10.1038/s41467-023-41391-7.

[52] Simon Andrews, FastQC: A quality control tool for high throughput sequence data, (n.d.). https://github.com/s-andrews/FastQC.

[53] A.M. Bolger, M. Lohse, B. Usadel, Trimmomatic: a flexible trimmer for Illumina sequence data, Bioinformatics 30 (2014) 2114–2120. https://doi.org/10.1093/bioinformatics/btu170.

[54] B. Langmead, S.L. Salzberg, Fast gapped-read alignment with Bowtie 2, Nat Methods 9 (2012) 357–359. https://doi.org/10.1038/nmeth.1923.

[55] Y. Liao, G.K. Smyth, W. Shi, The Subread aligner: fast, accurate and scalable read mapping by seed-and-vote, Nucleic Acids Res 41 (2013) e108. https://doi.org/10.1093/nar/gkt214.

[56] M.I. Love, W. Huber, S. Anders, Moderated estimation of fold change and dispersion for RNA-seq data with DESeq2, Genome Biol 15 (2014) 550. https://doi.org/10.1186/s13059-014-0550-8.

[57] Gene Ontology Consortium, The Gene Ontology resource: enriching a GOld mine, Nucleic Acids Res 49 (2021) D325–D334. https://doi.org/10.1093/nar/gkaa1113.

[58] C. Juillan-Binard, A. Picciocchi, J.-P. Andrieu, J. Dupuy, I. Petit-Hartlein, C. Caux-Thang, C. Vivès, V. Nivière, F. Fieschi, A Two-component NADPH Oxidase (NOX)-like System in Bacteria Is Involved in the Electron Transfer Chain to the Methionine Sulfoxide Reductase MsrP, J Biol Chem 292 (2017) 2485–2494. https://doi.org/10.1074/jbc.M116.752014.